The Astrophysical Journal, 720:912–922, 2010 September 1 doi:10.1088/0004-637X/720/1/912

FERMI LARGE AREA TELESCOPE OBSERVATIONS OF MISALIGNED ACTIVE GALACTIC NUCLEI

A. A. Abdo[1,2], M. Ackermann[3], M. Ajello[3], L. Baldini[4], J. Ballet[5], G. Barbiellini[6,7], D. Bastieri[8,9], K. Bechtol[3], R. Bellazzini[4], B. Berenji[3], R. D. Blandford[3], E. D. Bloom[3], E. Bonamente[10,11], A. W. Borgland[3], A. Bouvier[3], T. J. Brandt[12,13], J. Bregeon[4], A. Brez[4], M. Brigida[14,15], P. Bruel[16], R. Buehler[3], T. H. Burnett[17], S. Buson[8,9], G. A. Caliandro[18], R. A. Cameron[3], A. Cannon[19,20], P. A. Caraveo[21], S. Carrigan[9], J. M. Casandjian[5], E. Cavazzuti[22], C. Cecchi[10,11], Ö. Çelik[19,23,24], A. Celotti[25], E. Charles[3], A. Chekhtman[1,26], A. W. Chen[21], C. C. Cheung[1,2], J. Chiang[3], S. Ciprini[11], R. Claus[3], J. Cohen-Tanugi[27], S. Colafrancesco[22], J. Conrad[28,29,60], D. S. Davis[19,24], C. D. Dermer[1], A. de Angelis[30], F. de Palma[14,15], E. do Couto e Silva[3], P. S. Drell[3], R. Dubois[3], C. Favuzzi[14,15], S. J. Fegan[16], E. C. Ferrara[19], P. Fortin[16], M. Frailis[30,31], Y. Fukazawa[32], P. Fusco[14,15], F. Gargano[15], D. Gasparrini[22], N. Gehrels[19], S. Germani[10,11], N. Giglietto[14,15], P. Giommi[22], F. Giordano[14,15], M. Giroletti[33], T. Glanzman[3], G. Godfrey[3], P. Grandi[34,61], I. A. Grenier[5], J. E. Grove[1], L. Guillemot[35,36,37], S. Guiriec[38], D. Hadasch[39], M. Hayashida[3], E. Hays[19], D. Horan[16], R. E. Hughes[13], M. S. Jackson[29,40], G. Jóhannesson[3], A. S. Johnson[3], W. N. Johnson[1], T. Kamae[3], H. Katagiri[32], J. Kataoka[41], J. Knödlseder[12], M. Kuss[4], J. Lande[3], L. Latronico[4], S.-H. Lee[3], M. Lemoine-Goumard[36,37], M. Llena Garde[28,29], F. Longo[6,7], F. Loparco[14,15], B. Lott[36,37], M. N. Lovellette[1], P. Lubrano[10,11], G. M. Madejski[3], A. Makeev[1,26], G. Malaguti[34,61], M. N. Mazziotta[15], W. McConville[19,42], J. E. McEnery[19,42], P. F. Michelson[3], G. Migliori[25], W. Mitthumsiri[3], T. Mizuno[32], C. Monte[14,15,61], M. E. Monzani[3], A. Morselli[43], I. V. Moskalenko[3], S. Murgia[3], M. Naumann-Godo[5], I. Nestoras[35], P. L. Nolan[3], J. P. Norris[44], E. Nuss[27], T. Ohsugi[45], A. Okumura[46], N. Omodei[3], E. Orlando[47], J. F. Ormes[44], D. Paneque[3], J. H. Panetta[3], D. Parent[1,26], V. Pelassa[27], M. Pepe[10,11], M. Persic[6,31], M. Pesce-Rollins[4], F. Piron[27], T. A. Porter[3], S. Rainò[14,15], R. Rando[8,9], M. Razzano[4], S. Razzaque[1,2], A. Reimer[3,48], O. Reimer[3,48], L. C. Reyes[49], M. Roth[17], H. F.-W. Sadrozinski[50], D. Sanchez[16], A. Sander[13], J. D. Scargle[51], C. Sgrò[4], E. J. Siskind[52], P. D. Smith[13], G. Spandre[4], P. Spinelli[14,15], Ł. Stawarz[46,53], F. W. Stecker[19], M. S. Strickman[1], D. J. Suson[54], H. Takahashi[45], T. Tanaka[3], J. B. Thayer[3], J. G. Thayer[3], D. J. Thompson[19], L. Tibaldo[5,8,9,62], D. F. Torres[18,39], E. Torresi[34], G. Tosti[10,11,61], A. Tramacere[3,55,56], Y. Uchiyama[3], T. L. Usher[3], J. Vandenbroucke[3], V. Vasileiou[23,24], N. Vilchez[12], M. Villata[57], V. Vitale[43,58], A. P. Waite[3], P. Wang[3], B. L. Winer[13], K. S. Wood[1], Z. Yang[28,29], T. Ylinen[29,40,59], and M. Ziegler[50]

[1] Space Science Division, Naval Research Laboratory, Washington, DC 20375, USA
[2] National Research Council Research Associate, National Academy of Sciences, Washington, DC 20001, USA
[3] W. W. Hansen Experimental Physics Laboratory, Kavli Institute for Particle Astrophysics and Cosmology, Department of Physics and SLAC National Accelerator Laboratory, Stanford University, Stanford, CA 94305, USA
[4] Istituto Nazionale di Fisica Nucleare, Sezione di Pisa, I-56127 Pisa, Italy
[5] Laboratoire AIM, CEA-IRFU/CNRS/Université Paris Diderot, Service d'Astrophysique, CEA Saclay, 91191 Gif sur Yvette, France
[6] Istituto Nazionale di Fisica Nucleare, Sezione di Trieste, I-34127 Trieste, Italy
[7] Dipartimento di Fisica, Università di Trieste, I-34127 Trieste, Italy
[8] Istituto Nazionale di Fisica Nucleare, Sezione di Padova, I-35131 Padova, Italy
[9] Dipartimento di Fisica "G. Galilei," Università di Padova, I-35131 Padova, Italy
[10] Istituto Nazionale di Fisica Nucleare, Sezione di Perugia, I-06123 Perugia, Italy
[11] Dipartimento di Fisica, Università degli Studi di Perugia, I-06123 Perugia, Italy
[12] Centre d'Étude Spatiale des Rayonnements, CNRS/UPS, BP 44346, F-30128 Toulouse Cedex 4, France
[13] Department of Physics, Center for Cosmology and Astro-Particle Physics, The Ohio State University, Columbus, OH 43210, USA
[14] Dipartimento di Fisica "M. Merlin" dell'Università e del Politecnico di Bari, I-70126 Bari, Italy
[15] Istituto Nazionale di Fisica Nucleare, Sezione di Bari, 70126 Bari, Italy
[16] Laboratoire Leprince-Ringuet, École polytechnique, CNRS/IN2P3, Palaiseau, France
[17] Department of Physics, University of Washington, Seattle, WA 98195-1560, USA
[18] Institut de Ciencies de l'Espai (IEEC-CSIC), Campus UAB, 08193 Barcelona, Spain
[19] NASA Goddard Space Flight Center, Greenbelt, MD 20771, USA
[20] University College Dublin, Belfield, Dublin 4, Ireland
[21] INAF-Istituto di Astrofisica Spaziale e Fisica Cosmica, I-20133 Milano, Italy
[22] Agenzia Spaziale Italiana (ASI) Science Data Center, I-00044 Frascati (Roma), Italy
[23] Center for Research and Exploration in Space Science and Technology (CRESST) and NASA Goddard Space Flight Center, Greenbelt, MD 20771, USA
[24] Department of Physics and Center for Space Sciences and Technology, University of Maryland Baltimore County, Baltimore, MD 21250, USA
[25] Scuola Internazionale Superiore di Studi Avanzati (SISSA), 34014 Trieste, Italy
[26] George Mason University, Fairfax, VA 22030, USA
[27] Laboratoire de Physique Théorique et Astroparticules, Université Montpellier 2, CNRS/IN2P3, Montpellier, France
[28] Department of Physics, Stockholm University, AlbaNova, SE-106 91 Stockholm, Sweden
[29] The Oskar Klein Centre for Cosmoparticle Physics, AlbaNova, SE-106 91 Stockholm, Sweden
[30] Dipartimento di Fisica, Università di Udine and Istituto Nazionale di Fisica Nucleare, Sezione di Trieste, Gruppo Collegato di Udine, I-33100 Udine, Italy
[31] Osservatorio Astronomico di Trieste, Istituto Nazionale di Astrofisica, I-34143 Trieste, Italy
[32] Department of Physical Sciences, Hiroshima University, Higashi-Hiroshima, Hiroshima 739-8526, Japan
[33] INAF Istituto di Radioastronomia, 40129 Bologna, Italy
[34] INAF-IASF Bologna, 40129 Bologna, Italy
[35] Max-Planck-Institut für Radioastronomie, Auf dem Hügel 69, 53121 Bonn, Germany
[36] CNRS/IN2P3, Centre d'Études Nucléaires Bordeaux Gradignan, UMR 5797, Gradignan, 33175, France
[37] Université de Bordeaux, Centre d'Études Nucléaires Bordeaux Gradignan, UMR 5797, Gradignan, 33175, France
[38] Center for Space Plasma and Aeronomic Research (CSPAR), University of Alabama in Huntsville, Huntsville, AL 35899, USA
[39] Institució Catalana de Recerca i Estudis Avançats (ICREA), Barcelona, Spain

[40] Department of Physics, Royal Institute of Technology (KTH), AlbaNova, SE-106 91 Stockholm, Sweden
[41] Research Institute for Science and Engineering, Waseda University, 3-4-1, Okubo, Shinjuku, Tokyo, 169-8555 Japan
[42] Department of Physics and Department of Astronomy, University of Maryland, College Park, MD 20742, USA
[43] Istituto Nazionale di Fisica Nucleare, Sezione di Roma "Tor Vergata," I-00133 Roma, Italy
[44] Department of Physics and Astronomy, University of Denver, Denver, CO 80208, USA
[45] Hiroshima Astrophysical Science Center, Hiroshima University, Higashi-Hiroshima, Hiroshima 739-8526, Japan
[46] Institute of Space and Astronautical Science, JAXA, 3-1-1 Yoshinodai, Sagamihara, Kanagawa 229-8510, Japan
[47] Max-Planck Institut für extraterrestrische Physik, 85748 Garching, Germany
[48] Institut für Astro- und Teilchenphysik and Institut für Theoretische Physik, Leopold-Franzens-Universität Innsbruck, A-6020 Innsbruck, Austria
[49] Kavli Institute for Cosmological Physics, University of Chicago, Chicago, IL 60637, USA
[50] Santa Cruz Institute for Particle Physics, Department of Physics and Department of Astronomy and Astrophysics, University of California at Santa Cruz, Santa Cruz, CA 95064, USA
[51] Space Sciences Division, NASA Ames Research Center, Moffett Field, CA 94035-1000, USA
[52] NYCB Real-Time Computing Inc., Lattingtown, NY 11560-1025, USA
[53] Astronomical Observatory, Jagiellonian University, 30-244 Kraków, Poland
[54] Department of Chemistry and Physics, Purdue University Calumet, Hammond, IN 46323-2094, USA
[55] Consorzio Interuniversitario per la Fisica Spaziale (CIFS), I-10133 Torino, Italy
[56] INTEGRAL Science Data Centre, CH-1290 Versoix, Switzerland
[57] INAF, Osservatorio Astronomico di Torino, I-10025 Pino Torinese (TO), Italy
[58] Dipartimento di Fisica, Università di Roma "Tor Vergata," I-00133 Roma, Italy
[59] School of Pure and Applied Natural Sciences, University of Kalmar, SE-391 82 Kalmar, Sweden
Received 2010 April 22; accepted 2010 July 7; published 2010 August 13

ABSTRACT

Analysis is presented for 15 months of data taken with the Large Area Telescope (LAT) on the *Fermi Gamma-ray Space Telescope* for 11 non-blazar active galactic nuclei (AGNs), including seven FRI radio galaxies and four FRII radio sources consisting of two FRII radio galaxies and two steep spectrum radio quasars. The broad line FRI radio galaxy 3C 120 is reported here as a γ-ray source for the first time. The analysis is based on directional associations of LAT sources with radio sources in the 3CR, 3CRR, and MS4 (collectively referred to as 3C-MS) catalogs. Seven of the eleven LAT sources associated with 3C-MS radio sources have spectral indices larger than 2.3 and, except for the FRI radio galaxy NGC 1275 that shows possible spectral curvature, are well described by a power law. No evidence for time variability is found for any sources other than NGC 1275. The γ-ray luminosities of FRI radio galaxies are significantly smaller than those of the BL Lac objects detected by the LAT, whereas the γ-ray luminosities of the FRII sources are quite similar to those of FSRQs, which could reflect different beaming factors for the γ-ray emission. A core dominance (CD) study of the 3CRR sample indicates that sources closer to the jet axis are preferentially detected with the *Fermi* LAT, insofar as the γ-ray-detected misaligned AGNs have larger CD at a given average radio flux. The results are discussed in view of the AGN unification scenario.

Key words: galaxies: active – galaxies: jets – gamma rays: general

Online-only material: color figure

1. INTRODUCTION

The unification scenario (e.g., Urry & Padovani 1995) for active galactic nuclei (AGNs) explains a large variety of AGN properties in terms of the viewing angle toward a system consisting of an obscuring torus, an accretion disk providing fuel for a supermassive black hole, and broad- and narrow-line emission regions surrounding the black hole. Left unexplained is the dichotomy between radio-quiet and radio-loud AGNs. The latter objects contain jets of collimated plasma ejected with relativistic speeds transverse to the plane of the accretion disk. Such jets are very weak or absent in radio-quiet AGNs.

For the radio-loud AGNs, there are two main causes of anisotropy: the obscuring material of the torus that is roughly coplanar with and probably feeds the accretion disk, and the radio-emitting jets.

Decelerating jets and kilo-parsec scale edge-darkened lobes are found in the weaker FRI radio galaxies, while relativistic jets and edge-brightened radio lobes are found in the stronger FRII radio galaxies (Fanaroff & Riley 1974). According to the unification scenario, BL Lac objects and Flat Spectrum Radio Quasars (FSRQs) represent FRI and FRII radio galaxies, respectively, viewed nearly along the jet axis. In these sources, nonthermal radiation emitted from jets at the parsec scale is amplified by relativistic effects to produce flat radio spectrum sources with large optical polarization and strong optical variability, which furthermore are often found to exhibit superluminal motion in detailed radio monitoring. Sources with these attributes are collectively referred to as blazars. Multiwavelength observations show that blazars typically exhibit two-peaked broadband spectral energy distributions (SEDs) from radio to γ rays with the non-thermal electron-synchrotron radiation forming the lower-energy radio to X-ray emission, and Compton processes likely making the γ radiation (see, e.g., Böttcher 2007 for a review). Due to strong Doppler boosting, γ-ray blazars are detected from redshifts as large as $z \approx 3$ and with apparent γ-ray luminosities sometimes exceeding $\approx 10^{49}$ erg s^{-1}. The largest identified source population in the γ-ray sky are blazars (Hartman et al. 1999; Abdo et al. 2010a, 2010b).

By comparison, misaligned AGNs (MAGNs), with jets pointed away from the observer, are not favored GeV sources. By MAGNs we mean radio-loud AGNs with misdirected jets that display steep radio spectra ($\alpha_r \geqslant 0.5$, with the usual convention that $F_\nu \propto \nu^{-\alpha_r}$) and bipolar or quasi-symmetrical

[60] Royal Swedish Academy of Sciences Research Fellow, funded by a grant from the K. A. Wallenberg Foundation.
[61] Author to whom any correspondence should be addressed: grandi@iasfbo.inaf.it
[62] Partially supported by the International Doctorate on Astroparticle Physics (IDAPP) program.

Table 1
The Samples

Object	1FGL Name	R.A. (J2000)	Decl. (J2000)	Redshift	Class		log (CD) at 5 (GHz)	Ref.	Cat.
					Radio	Optical			
3C 78/NGC 1218	1FGLJ0308.3+0403	03 08 26.2	+04 06 39	0.029	FRI	G	−0.45	1	3CR
3C 84/NGC 1275	1FGLJ0319.7+4130	03 19 48.1	+41 30 42	0.018	FRI	G	−0.19	2[a]	3CR
3C 111	1FGLJ0419.0+3811	04 18 21.3	+38 01 36	0.049	FRII	BLRG	−0.3	3	3CRR
3C 120		04 33 11.1	+05 21 16	0.033	FRI	BLRG	−0.15	1	3CR
PKS 0625−354	1FGLJ0627.3−3530	06 27 06.7	−35 29 15	0.055	FRI[b]	G	−0.42	1	MS4
3C 207	1FGLJ0840.8+1310	08 40 47.6	+13 12 24	0.681	FRII	SSRQ	−0.35	2	3CRR
PKS 0943−76	1FGLJ0940.2−7605	09 43 23.9	− 76 20 11	0.27	FRII	G	<−0.56	4	MS4
M87/3C 274	1FGLJ1230.8+1223	12 30 49.4	+12 23 28	0.004	FRI	G	−1.32	2	3CRR
Cen A	1FGLJ1325.6−4300	13 25 27.6	− 43 01 09	0.0009[c]	FRI	G	−0.95	1	MS4
NGC 6251	1FGLJ1635.4+8228	16 32 32.0	+82 32 16	0.024	FRI	G	−0.47	2	3CRR
3C 380	1FGLJ1829.8+4845	18 29 31.8	+48 44 46	0.692	FRII/CSS	SSRQ	−0.02	2	3CRR

Notes.
[a] More recent 5 GHz core flux taken from Taylor et al. 2006. The CD value is uncertain because of the radio core variability.
[b] This source shows some BL Lac object characteristics in the optical band (see Wills et al. 2004).
[c] The Cen A distance is assumed to be 3.8 Mpc (Harris et al. 2009b).
References. (1) Morganti et al. 1993; (2) 3CRR database; (3) Linfield & Perley 1984; (4) Burgess & Hunstead 2006a, 2006b.

structures in radio maps. The larger jet inclination angle, in contrast with blazars, deboosts the radiation to make the relativistic jet radiation weaker than other potential sources of radio emission in these objects, such as synchrotron radiation from mildly relativistic outflows or extended radio lobe emission. The high-significance detections of NGC 1275 (Abdo et al. 2009a) and the Centaurus A radio galaxy confirming the EGRET result (Sreekumar et al. 1999; Abdo et al. 2010c, 2010d) in only 3 months of scientific observations with the *Fermi* Large Area Telescope (LAT; Atwood et al. 2009a) clearly show that misaligned radio-loud AGNs are another and potentially very interesting class of gamma-ray emitters. Indeed, several other MAGNs are listed in the first-year LAT AGN Catalog paper (1LAC; Abdo et al. 2010a). Very recently an LAT discovery of very high energy emission (>100 GeV) from the radio galaxy IC 310 has been reported (Neronov et al. 2010). This head-tail radio source, situated in the Perseus cluster, could belong to a new MAGN class of GeV emitters. The observed high energy photons could not originate in a jet but be produced at the bow shock formed by the interaction of the fast motion of the galaxy through the dense intercluster medium.

In this paper, we present a dedicated study of the γ-ray properties of all radio sources belonging to the Cambridge (3CR and 3CRR) and the Molonglo (MS4) catalogs associated with LAT detections in the first 15 months of sky survey, as described in Section 2. Our sample consists of 11 radio sources, all of which were reported in the 1LAC except for the radio galaxy 3C 120. LAT observations and analysis are described in Section 3, with results of the analysis given in Section 4. The properties of the MAGNs and *Fermi* LAT blazars are compared in Section 5, and the implications are discussed in Section 6. We conclude in Section 7.

In the following, we use a ΛCDM cosmology with values within 1σ of the *Wilkinson Microwave Anisotropy Probe* results (Komatsu et al. 2009); in particular, we use $h = 0.71$, $\Omega_m = 0.27$, and $\Omega_\Lambda = 0.73$, where the Hubble constant $H_0 = 100\,h$ km s^{-1} Mpc^{-1}.

2. THE SAMPLE

Our sample includes eleven MAGNs made up of nine radio galaxies, consisting of seven FRI and two FRII radio galaxies, and two steep spectrum radio quasars (SSRQs) with radio luminosities comparable to FRII sources. One of the two SSRQs, 3C 380, is sometimes classified as a compact steep spectrum (CSS) source, since most of its 5 GHz flux is emitted at galactic scales rather than at hundreds of kilo-parsec, as usually observed in FRII quasars (Wilkinson et al. 1991). In the unification scenario proposed for radio-loud AGNs, FRI and FRII radio galaxies are the parent population of BL Lac objects and FSRQs, respectively. The larger number, seven, of FRI sources compared to the four FRII objects may already reflect an interesting feature of the emission process insofar as BL Lac objects and FSRQs are about equally represented in the 1LAC (Abdo et al. 2010a).

With the exception of 3C 120, all of these sources are already reported in the 1LAC paper and have been established as associations by cross-correlating the one-year catalog sources with the 3CR catalog (Bennett 1962; Spinrad et al. 1985), the revised 3CRR catalog (Laing et al. 1983), and the Molonglo Southern 4 Jy Sample (MS4: Burgess & Hunstead 2006a, 2006b). These surveys are flux limited, with the 3CR, 3CRR, and MS4 flux limits of 9 Jy at 178 MHz, 10.9 Jy—also at 178 MHz, and 4 Jy at 408 MHz, respectively. The low-frequency selection criterion favors the detection of radio sources characterized by steep-spectrum synchrotron emission from extended lobes. Thus, the use of these catalogs (jointly referred to as the 3C-MS catalogs) for associations would preferentially select radio sources with large viewing angles. The 3C and 3CRR catalogs cover most part of the northern sky, with declination decl. $> -5^\circ$ and decl. $\geqslant 10^\circ$, respectively, while the MS4 catalog covers most of the southern sky, with $-85^\circ <$ decl. $< -30^\circ$. Finally, both optical and radio classifications are available for the majority of the sources. In particular, the 3CRR objects have been extensively studied from radio to X-rays.

LAT sources are positionally associated at high probability with the seven FRI radio galaxies and the two SSRQs and are included in the 1LAC (Table 1 in Abdo et al. 2010a). An LAT source is characterized by a high association probability ($P = 87\%$) with the FRII radio galaxy, 3C 111, but being located at low Galactic latitude, is not technically part of the 1LAC which is restricted to $|b| > 10^\circ$. It is, however, reported in Table 2 of the 1LAC. The other FRII radio galaxy, PKS 0943−76, is within the 95% error circle radius of 1FGL J0940.2−7605 and is considered a plausible association of the LAT γ-ray source,

and is listed among the AGN affiliations in Table 3 of the 1LAC paper. As its LAT association is less secure, we analyze the data of this radio galaxy keeping in mind its less secure association. Finally, we note that 3C 207 shows a very high association probability ($P = 99\%$) with 1FGL J0840.8+1310. Two other AGNs with association probabilities (51% and 71%) lower than those for 3C 207 are found within the 95% error radius. 3C 120 does not appear in the 1LAC, so we performed a new analysis now including all the available 15 month LAT data.

Table 1 gives the First Source Catalog (1FGL) LAT source name, probable associations, including their R.A. and decl.,[63] and redshift, radio (FRI, FRII, or CSS), optical (G—galaxy, BLRG–broad-line radio galaxy), and radio-optical (SSRQ—steep spectrum radio quasar) type of the MAGN sources. Also reported is the radio core dominance (CD) at 5 GHz. The CD value, considered a good indicator of the jet orientation, is defined as $\mathrm{CD} = \log(S_{\mathrm{core}}/[S_{\mathrm{tot}} - S_{\mathrm{core}}])$, where $S_{\mathrm{core/tot}}$ is the core/total flux density referred to the source rest frame (Scheuer & Readhead 1979). If we assume that the intrinsic power of the core is a fixed fraction f of the power of the extended components, CD is proportional to the beaming ($\mathrm{CD} = f\delta^{3+\alpha}$). If the bulk Lorentz factor (γ) of the emitting plasma is similar for all the sources with the same radio morphology, CD can be directly related to inclination angle θ. The CD parameter, however, suffers from several systematic uncertainties, for example, core variability, and radio map resolution, and sensitivity. Nevertheless, it provides a quantitative measure to directly connect observational quantities to AGN properties, in particular, beaming and inclination angle.

For the MAGNs quoted in Morganti et al. (1993) and Burgess & Hunstead (2006a, 2006b), the reported 5 GHz core fluxes density are K-corrected using $\alpha_{\mathrm{core}} = 0$, while for the extended component the correction has been performed using the spectral index listed in those papers. For all the other 3CRR objects in the sample, CD is calculated using the total 178 MHz flux, the 5 GHz core flux, and α_r between 178 and 750 MHz provided by the online 3CRR database.[64] The total 178 MHz flux density was converted into the total 5 GHz value following the method proposed by Fan & Zhang (2003). This approach made it possible to successively extend the CD study to the entire 3CRR sample (see Section 5).

3. LAT OBSERVATIONS AND DATA ANALYSIS

The *Fermi* LAT is a pair-conversion γ-ray telescope sensitive to photon energies from 20 MeV to >300 GeV. The LAT has a large peak effective area (~8000 cm^2 for 1 GeV photons in the event class considered here), viewing ~2.4 sr of the full sky with excellent angular resolution (68% containment radius better than ~1° at $E = 1$ GeV). It operates mainly in sky-survey mode, observing the entire sky every 3 hr. For a detailed description of the LAT, see Atwood et al. (2009).

We analyzed the LAT data collected during the first 15 months of operation, from 2008 August 4 to 2009 November 8. We kept only events in the "diffuse" class, with energies in the range 0.1–100 GeV, and with reconstructed zenith angle <105° in order to reduce the bright γ-ray albedo from the Earth. Also, we excluded the time intervals when the rocking angle was more than 52° and when the *Fermi* satellite was within the South Atlantic Anomaly. The standard *Fermi-LAT ScienceTools* software package[65] (version v9r15p5) was used with the P6_V3 set of instrument response functions. The spectral study was performed using the unbinned maximum-likelihood analysis implemented in the *gtlike* tool.

The model for which we calculated the likelihood is the combination of point-like and diffuse sources with a region of interest (RoI) having a radius of 12° and centered on the source under consideration. For each point-like source a power-law spectrum ($F = KE^{-\Gamma}$) derived from the *Fermi* LAT First Source Catalog (1FGL Catalog;[66] Abdo et al. 2010b) was adopted. Both parameters were allowed to vary freely. The local model for each RoI also includes sources falling between 12° and 19° of the target source, which can contribute at low energy due to the broad point-spread function (PSF). For these additional sources, spectral slopes and normalizations were fixed to the values provided by the 1FGL Catalog. As a further check, we repeated the same analysis using an RoI of 10°. In this case, all the sources falling between 10° and 15° were included and photon indices of the point-like sources fixed to 2. The two different approaches produced completely consistent results.

The background diffuse model used in the analysis is a combination of the Galactic emission model (gll_iem_v02.fit) and the extragalactic and instrumental background (isotropic_iem_v02.txt).[67] The background normalization was allowed to vary freely. The Galactic emission strongly affects analysis of sources located near the Galactic plane, as the diffuse background flux is very strong and structured, particularly below 1 GeV. In our sample, however, 3C 111 is the only source where the high Galactic background was important in the analysis.

The *gtlike* tool provides the best-fit parameters for each source and the significance of each source is given by the test statistic $\mathrm{TS} = 2\Delta\log(\mathrm{likelihood})$ between models with and without the source. When TS ⩽ 10, the flux values at $F > 100$ MeV are replaced by 2σ upper limits, derived by finding the point at which $2\Delta\log(\mathrm{likelihood}) = 4$ when increasing the flux from the maximum-likelihood value.

Once the likelihood analysis was performed on the entire 0.1–100 GeV band, this energy range was split into one, two, or three logarithmically spaced bins per decade, depending on the global flux of the source. The flux in each bin was obtained by fitting a power law, while keeping the spectral slope fixed at the value obtained by the fit in the entire energy range. As the considered energy bands are small, it can happen that a source has TS ⩽ 10 in more than one bin in spite of a relatively well constrained spectral shape on the overall 0.1–100 GeV band.

The departure of the source spectrum from a power law, obtained using the fluxes in the bins, was estimated using a χ^2 test following the procedure described in Abdo et al. (2010b).

The light curve of each source was generated dividing the total observation period in 15 and 5 time intervals of 1 month and 3 months duration, respectively, and repeating the likelihood analysis for each interval. The spectral index of each source was frozen to the best fit over the full interval with the exception of NGC 1275, for which both spectral parameters could also be well constrained in short time intervals. A standard χ^2 test was successively applied to the average flux in each light curve. We define a source as variable if the probability that its flux

[63] Coordinates from NASA/IPAC Extragalactic Database: NED.
[64] http://3crr.extragalactic.info/cgi/database
[65] http://fermi.gsfc.nasa.gov/ssc/data/analysis/documentation/Cicerone/
[66] http://fermi.gsfc.nasa.gov/ssc/data/access/lat/1yr_catalog/
[67] http://fermi.gsfc.nasa.gov/ssc/data/access/lat/BackgroundModels.html

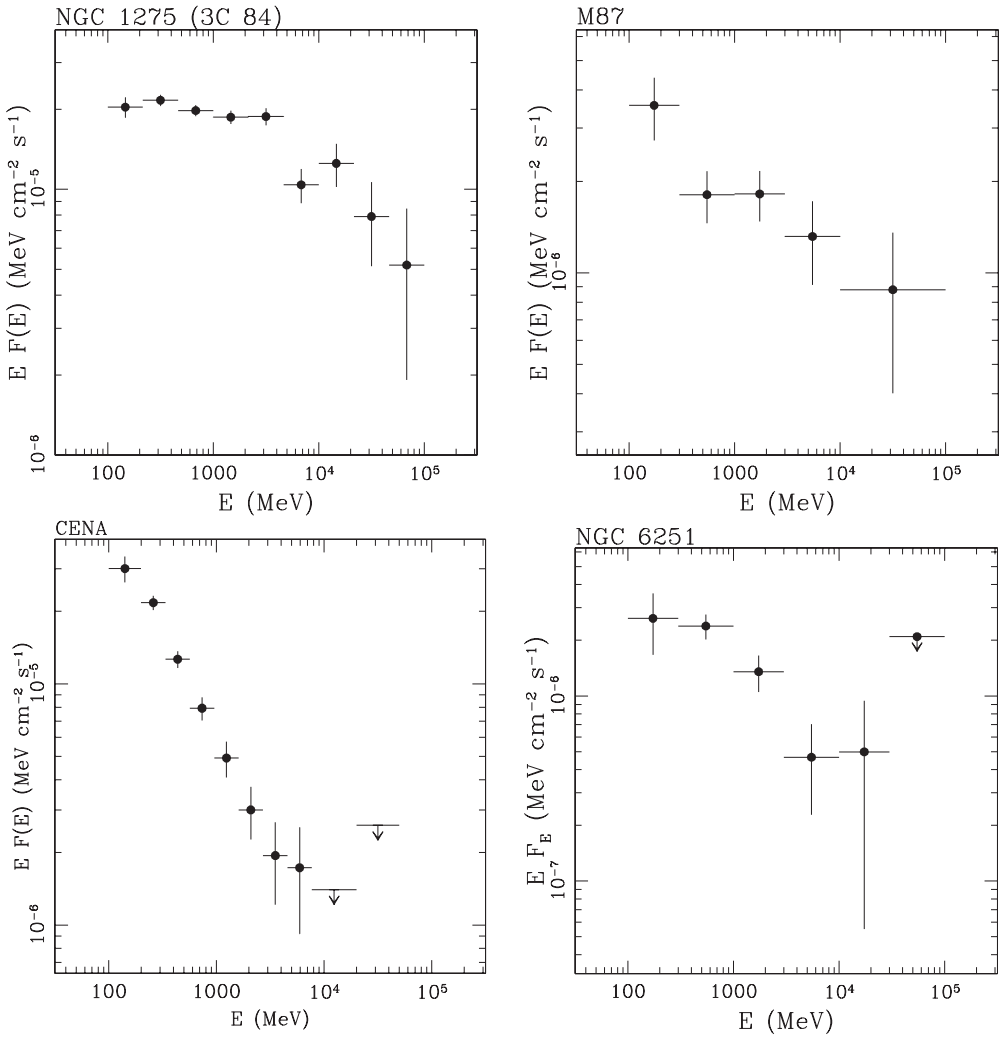

Figure 1. Spectral energy distributions (SEDs) of the FRI radio galaxies NGC 1275, M87, Cen A, and NGC 6251.

is constant is less than 10^{-3}. Note that all errors reported in the figures or quoted in the text are 1σ statistical errors. The estimated systematic errors on the flux, 10% at 100 MeV, 5% at 500 MeV, and 20% at 10 GeV, refer to uncertainties on the effective area of the instrument (see the 1FGL Catalog; Abdo et al. 2010b).

4. RESULTS

Table 2 summarizes the results of our analysis. For each source, the statistical significance over 15 months of observation is listed, in addition to the spectral parameters of the fitting technique described in the previous section. These include the power-law spectral slope, Γ, the integrated flux, $F(E > 100$ MeV), hereafter denoted as F_{100} in units of photons cm^{-2} s^{-1}, and the derived statistical uncertainties on these parameters. The K-corrected luminosity L_γ (erg s^{-1}) between $E_1 = 100$ MeV and $E_2 = 10$ GeV is calculated from the relation

$$L_\gamma = 1.6 \times 10^{-6} \times 4\pi d_L^2 E_1 \frac{(1-\Gamma)}{(2-\Gamma)} \frac{\left[\left(\frac{E_2}{E_1}\right)^{2-\Gamma} - 1\right]}{\left[\left(\frac{E100}{E_1}\right)^{1-\Gamma} - 1\right]} \times F_{100},$$

where d_L is the luminosity distance in cm, $E100$=100 GeV. Our results are consistent with those reported in the 1LAC catalog. Although not particularly bright, with average fluxes of $F_{100} \sim 6 \times 10^{-8}$, all sample sources have TS > 30, implying $\gtrsim 5\sigma$ detection. Note that the significance (TS) is dominated by 1–10 GeV photons (see also Figure 18, $d\mathrm{TS}/d\log E$ versus energy, in 1FGL paper) while the flux uncertainties by low energy events (characterized by a broad PSF and high background). This explains the presence in Table 2 of sources with high significance but large flux uncertainties.

The SEDs of the MAGNs are shown in Figures 1 and 2. Seven of the eleven sources have spectral slopes larger than 2.3, so that most photon energies lie between ≈ 100 MeV and 10 GeV. The spectrally softest case is 3C 120, from which only 100 MeV–1 GeV emission is detected. In spite of its faintness, the detection of 3C 120 is however significant at $\approx 5.6\sigma$ (Table 2). Its analysis was performed following the standard procedure but with its position fixed to the optical nuclear coordinates. Although 3C 120 could be slightly contaminated by the nearby FSRQ 1FGL J0427.5+0515, we estimate that the effect is negligible, since the two sources are 1.°4 apart and clearly resolved in the count map (Figure 3). Only two FRI radio galaxies, 3C 78 and PKS 0625−354, are not detected at energies $\lesssim$300 MeV and show rather noisy spectra. These are the weaker sources in the sample with $F_{100} < 10^{-8}$. Indeed, for PKS 0625−354 we were forced to restrict the likelihood analysis to the 300 MeV–100 GeV band in order to constrain the spectral parameters. Due to the low quality of the data, the

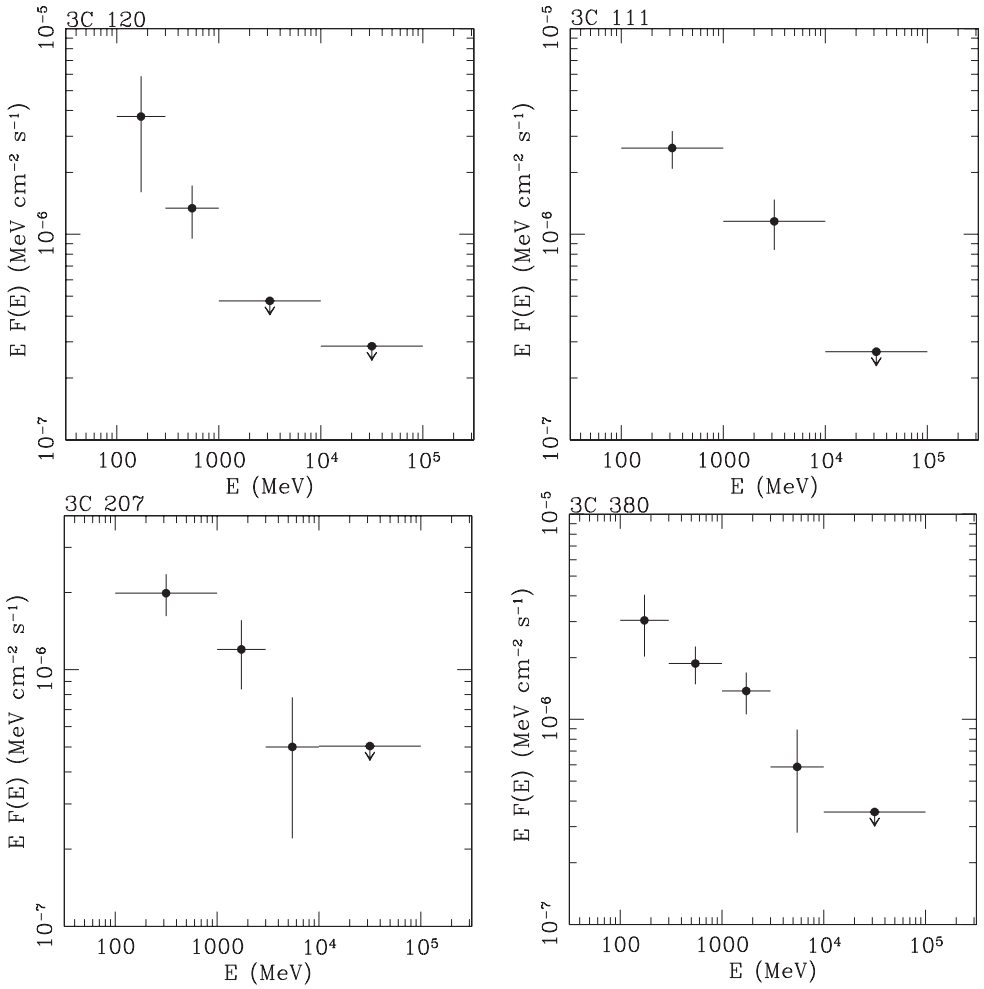

Figure 2. SEDs of the two BLRGs 3C 120 and 3C 111 (upper panel) and of the two steep spectrum radio quasars 3C 207 and 3C 380 (lower panel).

SEDs of 3C 78 and PKS 0625−354 are not shown in Figure 1. 3C 111 is another source for which it was necessary to perform a more accurate analysis. As already mentioned, this radio galaxy is located at low Galactic latitude and is affected by high background. In addition, it was probably in a high state only for a short time during the 15 months of integration (as briefly discussed later). As the source was below the LAT detection threshold for most of the time, a 15 month integration time necessarily reduces the source excess counts. Therefore, in order to constrain Γ, all the spectral parameters of the sources within the RoI were initially fixed. Successively, the uncertainty in F_{100} was estimated by freezing the spectral slope of the target and allowing the normalization and slope of the other point-like sources to vary.

NGC 1275 is the only source showing a complex spectral shape (see Figure 1), based on the data set that is larger than the one used in the 4 month analysis in the original discovery paper, where a power-law fit was acceptable (Abdo et al. 2009b). When a power law is applied to the data, the probability that the model is adequate is small, with $P_{\chi^2} = 0.012$, corresponding to $\chi^2 = 18$ for 7 degrees of freedom (dof). This radio galaxy is also characterized by flux and spectral variability (see Figure 4). According to the χ^2 statistics, the model of constant flux ($\chi^2 = 54$ for 4 dof) as well as the model of constant spectral shape ($\chi^2 = 28$ for 4 dof) can be ruled out. A detailed analysis of the spectral evolution of NGC 1275 can be found in Kataoka et al. (2010).

Table 2
Results of the *Fermi* LAT Analysis

Object	TS	Γ	Flux[a] (>100 MeV)	logLum[b] (0.1–10 GeV)
3C 78/NGC 1218	35	1.95 ± 0.14	4.7 ± 1.8	42.84
3C 84/NGC 1275	4802	2.13 ± 0.02	222 ± 8	44.00
3C 111	34	2.54 ± 0.19	40 ± 8[c]	44.00
3C 120	32	2.71 ± 0.35	29 ± 17	43.43
PKS 0625−354[d]	97	2.06 ± 0.16	4.8 ± 1.1	43.7
3C 207	79	2.42 ± 0.10	24 ± 4	46.44
PKS 0943−76	65	2.83 ± 0.16	55 ± 12	45.71
M87/3C 274	194	2.21 ± 0.14	24 ± 6	41.67
Cen A	1010	2.75 ± 0.04	214 ± 12	41.13
NGC 6251	143	2.52 ± 0.12	36 ± 8	43.30
3C 380	95	2.51 ± 0.30	31 ± 18	46.57

Notes.
[a] $\times 10^{-9}$ photon cm^{-2} s^{-1}.
[b] erg s^{-1}.
[c] Flux was estimated keeping the spectral slope fixed.
[d] Likelihood analysis was limited to the 300 MeV–100 GeV range. Flux (>300 MeV); luminosity extrapolated down to 100 MeV.

Although bright enough to be detected in each temporal bin, no evidence for variability was found in our analysis of M87, Cen A, and NGC 6251. However, small statistics prevent us

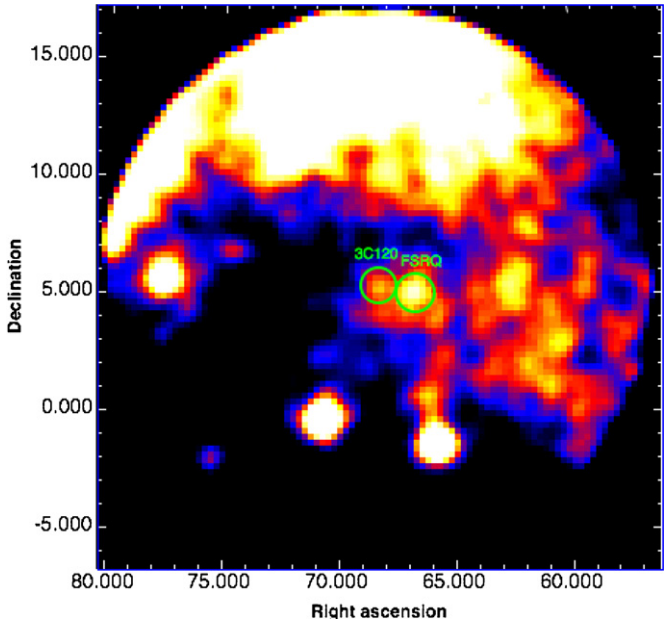

Figure 3. 3C 120 count sky map between 100 MeV and 100 GeV.
(A color version of this figure is available in the online journal.)

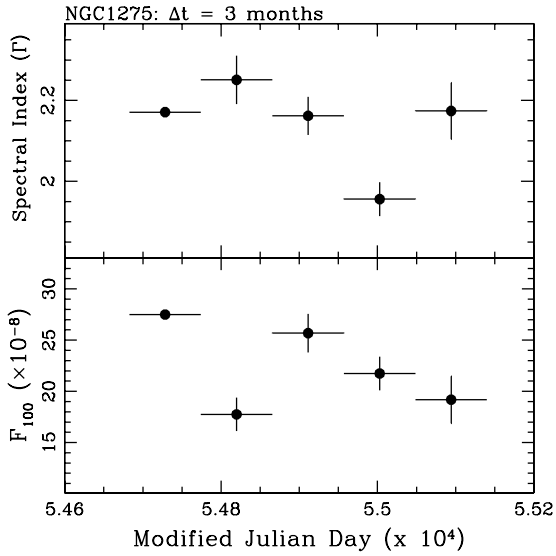

Figure 4. Flux and spectral slope variations of NGC 1275. Each bin corresponds to 3 months of observations in the 100 MeV–100 GeV band.

from detecting factor of 2 flux changes. Incidentally, we note that NGC 6251 was observed by EGRET in a brighter flux state ($F_{100} = (74 \pm 23) \times 10^{-9}$), suggesting a possible γ-ray variability of this source on timescales of years (Hartman et al. 1999; Mukherjee et al. 2002).

The other sources were not significant in each time interval. For example, 3C 111 and 3C 120 (Figures 5 and 6) reached the minimal significance required for detection (TS >10) in only one occasion, even considering a bin integration time of 3 months. In the case of 3C 111 a low duty cycle for γ-ray emission was also suggested by Hartman et al. (2008). They noted that this source only occasionally became bright ($F_{100} > 10^{-7}$) and detectable by EGRET. The difference in flux between EGRET and *Fermi* detections suggests evidence for long term variability.

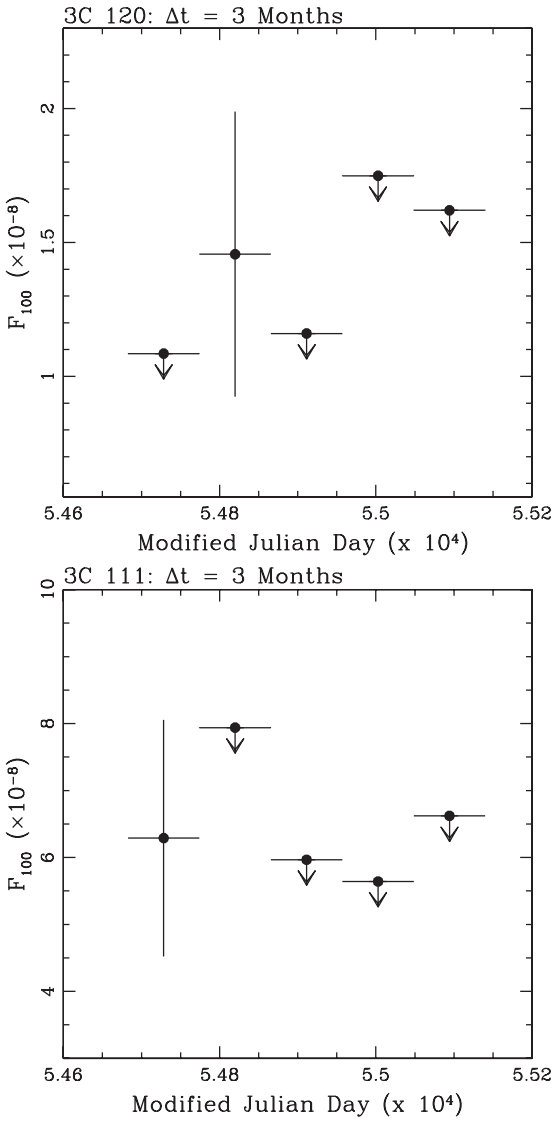

Figure 5. Light curves of the broad line radio galaxies 3C 120 and 3C 111 between 100 MeV and 100 GeV. Each bin covers 3 months of observations.

5. COMPARISON WITH *FERMI* LAT BLAZARS

5.1. The Γ–L_γ Plane

The spectral slope Γ as a function of 0.1–10 GeV γ-ray luminosity L_γ for all the sources of our sample is plotted in Figure 6, along with the corresponding values for FSRQs and BL Lac objects from the 1LAC.

As can be seen, MAGNs and blazars occupy different regions of the Γ–L_γ plane. The MAGNs are less luminous on average than the γ-ray blazars. When a Kolmogorov–Smirnov test is applied, the associated probability that blazars and MAGNs are drawn from the same population is $P_{\rm KS} < 10^{-3}$. Although a range of intrinsic source luminosities cannot be excluded, this result is in rough accordance with expectations from unified scenarios insofar as jets that are not directly pointed toward the observer are expected to be fainter because of the smaller Doppler boosting.

The difference between properties of BL Lac objects and FSRQs on the one hand, and FRI radio galaxies and FRII sources on the other, is also evident in Figure 7 where a histogram of the γ-ray luminosities of the FRI radio galaxies and the FRII

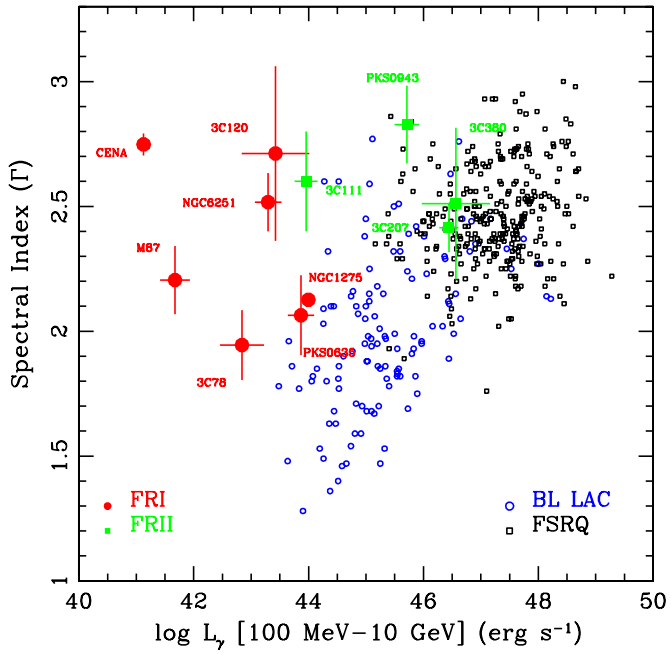

Figure 6. Spectral slopes of FRI radio galaxies (red circles), FRII radio sources (green squares), BL Lac objects (open blue circles), and FSRQs (open black squares) are plotted as a function of the γ-ray luminosity (100 MeV–10 GeV). Local radio galaxies ($z < 0.1$) and blazars occupy different regions of the plot, with misaligned AGNs generally characterized by lower luminosity. On the contrary, the two more distant steep spectrum radio quasars ($z > 0.6$) fall within the range of γ-ray luminosities of FSRQs.

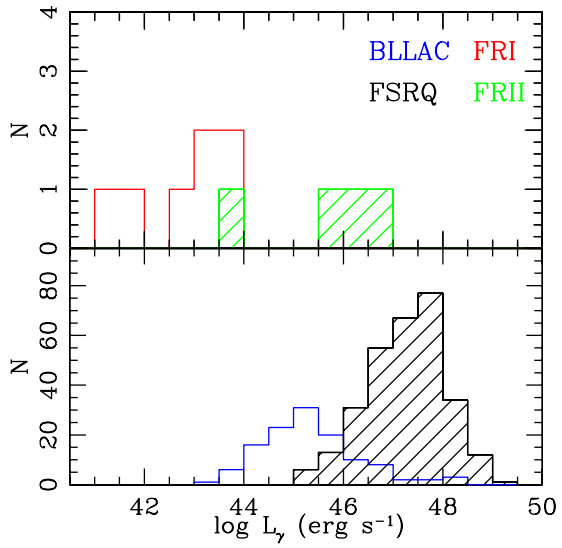

Figure 7. Histogram showing the luminosity distribution of misaligned AGNs (upper panel : FRIs—red continuum line, FRIIs—green dashed line) and blazars (lower panel: BL Lac objects—blue continuum line; FSRQs—black dashed line). FRI radio galaxies are significantly less luminous than BL Lac objects. The broad-line radio galaxy 3C 111 is the only FRII outside the luminosity range covered by the FSRQ

sources (upper panel) and the BL Lac objects and FSRQs (lower panel) in the 1LAC are shown. Inspection of Figures 6 and 7 shows a well defined separation between FRIs and BL Lac objects, their putative parent population. On the contrary, FRIIs seem to lie at best in the outskirts of the FRSQ distribution. Although care must be taken when drawing conclusions due to the small statistics and about PKS 0943−76 because of the uncertainty that the *Fermi* γ-ray source is correctly associated with it (Section 2), a tentative conclusion implied is that the range of γ-ray luminosities of FRI radio galaxies compared to BL Lac objects is larger than that of the FRII galaxies compared to FSRQs.

The significance of this result, if validated with greater statistics as the *Fermi* mission progresses, is considered in Section 6.

5.2. Core Dominance Study of the 3CRR Sample

In order to better understand the nature of the γ-ray emitting MAGNs, we considered the flux-limited 3CRR sample and analyzed the role of CD (defined in Section 2), of individual sources that were detected with the *Fermi* LAT compared with those that were not detected. We choose the 3CRR sample because it is well studied and contains the most complete set of data available for such a study. Because it is restricted to the northern sky, not all the MAGNs in our study are considered.

Figure 8 shows CD as a function of the total flux density at 178 MHz. In this plot, γ-ray emitters are identified by triangles inside the filled circles. The plot clearly shows that at a given radio flux, radio galaxies, and quasars detected at MeV–GeV energies have the largest CD values. In other words, LAT preferentially selects the misaligned AGNs with smaller angles of inclination. The MAGNs radiating at GeV energies do not, however, share the extreme CD values of blazars. To

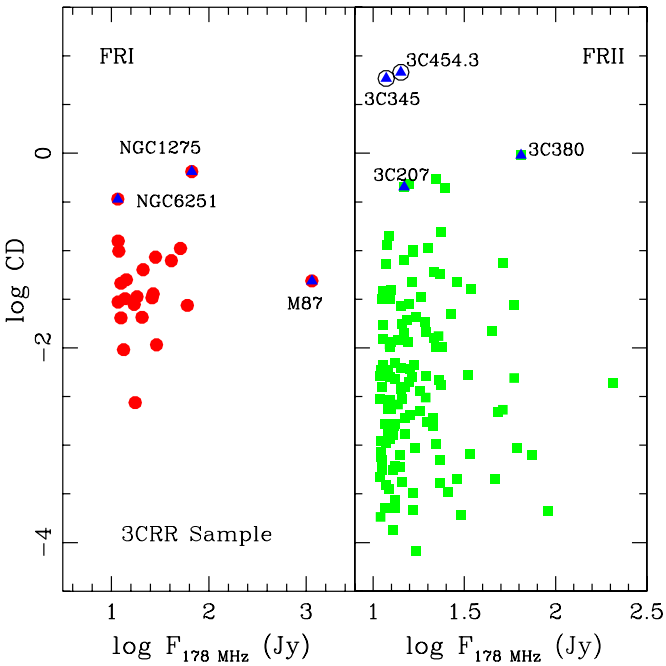

Figure 8. Core dominance (CD) vs. total flux at 178 MHz of all the sources of the 3CRR sample (FRI—red circles; FRII—green squares) with a measured radio core. The MAGNs detected by *Fermi* (blue triangles in circles/squares) are characterized by large CDs. The two FSRQs (blue triangles in empty black circles) belonging to the 3CRR and associated with LAT sources have much larger CD values than the misaligned FRII sources.

demonstrate this, we show the CD values for two FSRQs, 3C 454.3 and 3C 345, which are associated with *Fermi* LAT sources, belong to the 3CRR sample, and are denoted by the blue triangles in black circles in Figure 8 (right panel). These sources occupy the upper region of the CD/$F_{178\,\mathrm{MHz}}$ plane, much greater than the values for the misaligned FRII γ-ray sources (which are both, incidentally, the SSRQs). A similar plot can be obtained by considering the 5 GHz core flux, rather than the total radio emission.

Considering all the FRI γ-ray sources listed in Table 1, in particular those shown in Figure 8 (left panel), it appears that FRI radio galaxies with large jet inclination angles and correspondingly small CDs can be observed only if nearby, that is, if they have large radio flux densities. When the distance increases, the source flux becomes weaker, so for them to be detectable at GeV energies the CD must increase.

No FRII radio galaxy observed at large angles to the jet axis as reflected by a small CD parameter has yet been detected with *Fermi*. That we have yet to detect FRIIs with small CD would simply be a consequence of FRIIs being at larger redshifts than FRIs and thus too weak to be detected. Indeed, the median of the 3CRR redshift distribution for FRI and FRII radio galaxies is $z = 0.03$ and $z = 0.56$, respectively. The narrow line radio galaxy (NLRG) Cygnus A, which is an FRII at $z = 0.056$, exhibits a large core radio flux ($F_c \sim 700$ mJy at 5 GHz; Hardcastle et al. 2004), of the same order as Cen A. So far, it is not detected with the *Fermi* LAT. Both objects are seen at large inclination angles, yet both the core and lobes of Cen A are detected (Abdo et al. 2010c, 2010d). If proportionality between core radio and γ-ray flux is assumed (see, for example, Giroletti et al. 2010), the origin of the different γ-ray behaviors may reside in the different jet structure. While the Cen A jet could be either decelerating or surrounded by slower external layers, Cygnus A might have a collimated relativistic jet with a slower sheath.

6. DISCUSSION

Following the Fanaroff & Riley (1974) classification, we have assigned the MAGNs into two radio morphological classes corresponding to edge-darkened (FRI) and edge-brightened (FRII) objects, with FRII objects being more powerful ($P_{178\,\mathrm{MHz}} > 10^{25}$ W Hz^{-1} sr^{-1}) than FRI radio galaxies. In the FRIs, the jets are thought to decelerate and become sub-relativistic on scales of hundreds of pc to kpc, while the jets in FRIIs are at least moderately relativistic and supersonic from the core to the hot spots. The nuclei of FRIs are not generally absorbed and are probably powered by inefficient accretion flows (e.g., Chiaberge et al. 1999; Balmaverde et al. 2006). On the contrary, most FRIIs are thought to have an efficient engine and a dusty torus (e.g., Belsole et al. 2006).

From the optical point of view, FRII radio galaxies with bright continuum and broad optical emission lines are classified as broad-line radio galaxies (BLRGs). They are classified as narrow line radio galaxies (NLRGs)[68] if their continuum is weak and only narrow emission lines are observed. In the framework of blazar unification, the transition from NLRGs to BLRGs would represent the increasing alignment of the observer along the jet axis. An MAGN is defined as a quasar if its integrated optical luminosity is dominated by a point-like source rather than by the host galaxy. SSRQs would be high luminosity counterparts of BLRGs.

Assuming isotropic emission in the comoving jet frame with a power-law spectrum of index α, the observed flux density $F(\nu)$ produced through synchrotron and synchrotron self-Compton (SSC) emission is related to the rest-frame flux density $F'(\nu')$ through the relation $F(\nu) = \delta^{3+\alpha} F'(\nu)$, where δ is the Doppler factor defined by $\delta = [\gamma(1 - \beta\cos\theta)]^{-1}$, and $\nu = \delta\nu'/(1 + z)$. Here, βc is the bulk velocity of the emitting plasma, $\gamma = (1 - \beta^2)^{-1/2}$ is the corresponding Lorentz factor, and θ is the jet viewing angle (Urry & Padovani 1995). A radio-loud AGN with $\alpha \approx 1$ and $\gamma \approx 10$ would then have a flux density at $\theta \sim 10^\circ$ smaller than an aligned blazar by a factor ≈ 250. The Doppler boosting is stronger and the γ-ray beaming cone narrower compared to synchrotron processes if the emission is due to Compton scattering of external photons (EC) in the jet. In this case, the beaming factor of the flux density varies by a factor of $\delta^{4+2\alpha}$ (Dermer 1995), or a factor $\delta^{1+\alpha}$ times the synchrotron beaming factor.

Although the number of sources is small, the behavior shown in Figure 6 could be explained if the γ-ray beaming cones are narrower in FRII sources, relative to the radio synchrotron beaming cones, than in FRI sources. This is consistent with the beaming factors just described, provided that the γ-ray emission from FRIIs originates from EC processes, as would be expected since these sources have prominent broad line regions. In this case, the stronger reduction in the EC flux for FRII radio galaxies viewed slightly away from the jet axis ($\theta \gtrsim 1/\Gamma$) as compared to the SSC flux for off-axis FRI radio galaxies makes the detection of off-axis FRI galaxies more probable. This is in accordance with statistical models (Mücke & Pohl 2000; Dermer 2007) of radio galaxies and blazars that predicted a larger number of FRI than FRII radio galaxies would be detected by *Fermi* due to the different beaming factors.

However, the situation is undoubtedly more complicated. First note that given the strong Doppler boosting of the jetted radiations from blazars, the EGRET detection of the radio galaxies Cen A and NGC 6251 (Sreekumar et al. 1999; Mukherjee et al. 2002) is already somewhat surprising. SEDs of FRI radio galaxies such as NGC 1275 (Abdo et al. 2009b) and M87 (Abdo et al. 2009c) are consistent with an SSC model with Γ (and δ) $\lesssim 3$, which are much lower than typical values found in models of BL Lac objects (e.g., Costamante & Ghisellini 2002; Finke et al. 2008). The corresponding off-axis synchrotron and Compton fluxes imply a slower bulk velocity of the emitting plasma for the viewing angles inferred by very long baseline interferometry observations; otherwise the debeamed radiation would be much weaker than observed (Guainazzi et al. 2003; Chiaberge et al. 2000, 2001, 2003; Foschini et al. 2005). This has led to the development of complex models for the structure of the jet, including decelerating jet flows (Georganopoulos & Kazanas 2003) and the spine-layer jet model (Stawarz & Ostrowski 2002; Ghisellini et al. 2005). A possible spine-layer morphology of the jet is also supported by earlier radio-optical observations concerning polarization properties and intensity brightness profiles in both FRI and FRII sources (e.g., Owen et al. 1989; Laing 1996; Swain et al. 1998; Attridge et al. 1999), as well as by numerical simulations of relativistic flows (e.g., Aloy et al. 1999; Rossi et al. 2008).

In the MAGN sources that do not exhibit strong evidence for variability (all except NGC 1275), the observed γ-ray emission could be made in regions well beyond the parsec scale. For example, a slowly varying, high-energy emission component can be formed by Compton-scattered ambient photon fields, including the cosmic microwave background radiation (Böttcher et al. 2008). Proton synchrotron radiation from ultra-relativistic protons in the milligauss fields of knots and hot spots could also be made at kilo-parsec scales from the nuclei of radio galaxies (Aharonian 2002). Rapid variability does not necessarily exclude emission from sites outside the pc-scale core, as indicated in X-ray studies of M87 (Cheung et al. 2007; Harris et al. 2009a) and Pictor A (Marshall et al. 2010). A detailed statistical study of *Fermi* AGNs will be required to test blazar unification, rule

[68] With NLRGs we only consider FRII radio galaxies with high excitation lines, characterized by an [O III] equivalent width larger than 10 Å and/or an [O II]/[O III] ratio larger than 1 (Jackson & Rawlings 1997).

out simple one-zone models, and determine the location of the emission region.

We note that the possible detection of several FRIs and some BLRGs at GeV energies had already been predicted before the *Fermi* launch. In particular, see the papers by Stawarz et al. (2003, 2006), Ghisellini et al. (2005), and Grandi & Palumbo (2007).

7. SUMMARY AND CONCLUSIONS

We have presented an analysis of 15 months of LAT data for 11 radio sources listed in the low radio frequency 3CRR, 3CR, and MS4 catalogs. In addition to BL Lac object and FSRQ blazars, misaligned radio sources represent a new and important class of GeV emitters. Among the misaligned AGNs studied in this paper, Cen A, NGC 6251, and 3C 111 are the only radio galaxies that were EGRET candidate sources (Sreekumar et al. 1999; Mattox et al. 2001; Mukherjee et al. 2002; Sowards-Emmerd et al. 2003; Sguera et al. 2005; Hartman et al. 2008). The other eight objects represent new discoveries made with the *Fermi* LAT. Dedicated papers have been recently published or are in preparation on three of these, namely, NGC 1275 (Abdo et al. 2009b), M87 (Abdo et al. 2009c), and Cen A (Abdo et al. 2010c, 2010d).

The following points outline our results and conclusions.

1. Our sample is dominated by seven nearby ($d \lesssim 250$ Mpc) FRI radio galaxies. Four FRII radio sources, including two FRII radio galaxies and two SSRQs, are associated with LAT sources at high probability. The most distant MAGNs are the SSRQs, at $z \approx 0.7$.
2. The misaligned FRII sources, though few in number, are somewhat less γ-ray luminous than their parent population of FSRQs, but have comparable average γ-ray spectral indices. The FRI radio galaxies are significantly less luminous than their parent population of BL Lac objects, in accordance with the unification scenario for radio galaxies and blazars. The SSRQs appear very similar to γ-ray emitting FSRQs, suggesting a more powerful Doppler boosting when compared with radio galaxies.
3. A simple power law is a good representation of the 15 month data except for NGC 1275, the brightest source in the sample, which requires a spectral softening above ≈ 3 GeV. NGC 1275 is also the only MAGN for which variability on timescales of months is measured. Comparison between *Fermi* and EGRET fluxes suggests variability on a timescale of years for NGC 6251 and 3C 111, in addition to NGC 1275.
4. The CD of the 3CRR sample, which includes five MAGNs, indicates that *Fermi* preferentially detects radio sources intermediate between blazars and radio galaxies with large jet inclinations to the line of sight. Only the very nearby radio galaxies M87 and Cen A have small CD and large jet angles, suggesting that their detection is in large part a consequence of their proximity. MAGNs at larger distances have larger values of CD.
5. The small number of FRIIs with LAT associations could be due to the fewer nearby FRII than FRI sources, and to different beaming factors of the emission in the jets of FRII and FRI radio galaxies.

As the *Fermi* mission continues, more detections of radio galaxies and misaligned AGNs can be expected. Joint statistical analysis of *Fermi* AGNs will test the unification hypothesis of radio galaxies and blazars, models for jet structure and γ-ray beaming, and the contribution of MAGNs to the extragalactic γ-ray background radiation. Such studies could help explain the reason for the difference between radio-loud and radio-quiet AGNs.

The *Fermi* LAT Collaboration acknowledges generous ongoing support from a number of agencies and institutes that have supported both the development and the operation of the LAT as well as scientific data analysis. These include the National Aeronautics and Space Administration and the Department of Energy in the United States; the Commissariat à l'Energie Atomique and the Centre National de la Recherche Scientifique/Institut National de Physique Nucléaire et de Physique des Particules in France; the Agenzia Spaziale Italiana and the Istituto Nazionale di Fisica Nucleare in Italy; the Ministry of Education, Culture, Sports, Science and Technology (MEXT), High Energy Accelerator Research Organization (KEK), and Japan Aerospace Exploration Agency (JAXA) in Japan; and the K. A. Wallenberg Foundation, the Swedish Research Council, and the Swedish National Space Board in Sweden.

Additional support for science analysis during the operations phase is gratefully acknowledged from the Istituto Nazionale di Astrofisica in Italy and the Centre National d'Études Spatiales in France.

This research has made use of the NASA/IPAC Extragalactic Database (NED) which is operated by the Jet Propulsion Laboratory, California Institute of Technology, under contract with the National Aeronautics and Space Administration.

REFERENCES

Abdo, A. A., et al. 2009a, ApJ, 700, 597 (LBAS)
Abdo, A. A., et al. 2009b, ApJ, 699, 31 (NGC 1275)
Abdo, A. A., et al. 2009c, ApJ, 707, 55 (M87)
Abdo, A. A., et al. 2010a, ApJ, 715, 429 (1LAC)
Abdo, A. A., et al. 2010b, ApJS, 188, 405 (1FGL)
Abdo, A. A., et al. 2010c, Science, 328, 725 (Cen A Lobes)
Abdo, A. A., et al. 2010d, ApJ, 719, 1433 (Cen A core)
Aharonian, F. A. 2002, MNRAS, 332, 215
Aloy, M. A., et al. 1999, ApJ, 523, L125
Attridge, J. M., Roberts, D. H., & Wardle, J. F. 1999, ApJ, 518, L87
Atwood, W. B., et al. 2009, ApJ, 697, 1071
Balmaverde, B., Capetti, A., & Grandi, P. 2006, A&A, 451, 351
Belsole, E., Worrall, D. M., & Hardcastle, M. J. 2006, MNRAS, 366, 339
Bennett, A. S. 1962, MNRAS, 125, 75
Böttcher, M. 2007, in ASP Conf. Ser. 373, The Central Engine of Active Galactic Nuclei, ed. L. C. Ho & J-M Wang (San Francisco, CA: ASP), 169
Böttcher, M., Dermer, C. D., & Finke, J. D. 2008, ApJ, 679, L9
Burgess, A. M., & Hunstead, R. W. 2006a, AJ, 131, 100
Burgess, A. M., & Hunstead, R. W. 2006b, AJ, 131, 114
Cheung, C. C., Harris, D. E., & Stawarz, Ł. 2007, ApJ, 663, L65
Chiaberge, M., Capetti, A., & Celotti, A. 1999, A&A, 349, 77
Chiaberge, M., Capetti, A., & Celotti, A. 2001, MNRAS, 324, 33
Chiaberge, M., Gilli, R., Capetti, A., & Macchetto, F. D. 2003, ApJ, 597, 166
Chiaberge, M., et al. 2000, A&A, 358, 104
Costamante, L., & Ghisellini, G. 2002, A&A, 384, 56
Dermer, C. D. 1995, ApJ, 446, L63
Dermer, C. D. 2007, ApJ, 659, 958
Fan, J. H., & Zhang, J. S. 2003, A&A, 407, 899
Fanaroff, B. L., & Riley, J. M. 1974, MNRAS, 167, 31
Finke, J. D., Dermer, C. D., & Böttcher, M. 2008, ApJ, 686, 181
Foschini, L., et al. 2005, A&A, 433, 515
Georganopoulos, M., & Kazanas, D. 2003, ApJ, 589, L5
Ghisellini, G., Tavecchio, F., & Chiaberge, M. 2005, A&A, 432, 401
Giroletti, M., et al. 2010, Fermi Symposium, eConf Proceedings C091122 (arXiv:1001.5123)
Grandi, P., & Palumbo, G. G. C. 2007, ApJ, 659, 235
Guainazzi, M., Grandi, P., Comastri, A., & Matt, G. 2003, A&A, 410, 131
Hardcastle, M. J., et al. 2004, ApJ, 612, 729

Harris, D. E., Cheung, C. C., Stawarz, Ł., Biretta, J. A., & Perlman, E. S. 2009a, ApJ, 699, 305
Harris, G. L.-H., Rejkuba, M., & Harris, W. E. 2009b, PASA, in press (arXiv:0911.318)
Hartman, R. C., Kadler, M., & Tueller, J. 2008, ApJ, 688, 852
Hartman, R. C., et al. 1999, ApJS, 123, 79
Jackson, N., & Rawlings, S. 1997, MNRAS, 284, 241
Kataoka, J., et al. 2010, ApJ, 715, 554
Komatsu, E., et al. 2009, ApJS, 180, 330
Laing, R. A. 1996, in ASP Conf. Ser. 100, Energy Transport in Radio Galaxies and Quasars, ed. P. E. Hardee, A. H. Bridle, & Z. J. Anton (San Francisco, CA: ASP), 241
Laing, R. A., Riley, J. M., & Longair, M. S. 1983, MNRAS, 204, 151
Linfield, R., & Perley, R. 1984, ApJ, 279, 60
Marshall, H. L., et al. 2010, ApJ, 714, L213
Mattox, J. R., Hartman, R. C., & Reimer, O. 2001, ApJS, 135, 155
Morganti, R., Killeen, N. E. B., & Tadhunter, C. N. 1993, MNRAS, 263, 1023
Mücke, A., & Pohl, M. 2000, MNRAS, 312, 177
Mukherjee, R., Halpern, J., Mirabal, N., & Gotthelf, E. V. 2002, ApJ, 574, 693
Neronov, A., Semikoz, D., & Vovk, Ie. 2010, A&A, in press (arXiv:1003.4615)
Owen, F. N., Hardee, P. E., & Cornwell, T. J. 1989, ApJ, 340, 698
Rossi, P., et al. 2008, A&A, 488, 795
Scheuer, P. A. G., & Readhead, A. C. S. 1979, Nature, 277, 182
Sguera, V., et al. 2005, A&A, 430, 107
Sowards-Emmerd, D., Romani, R. W., & Michelson, P. F. 2003, ApJ, 590, 109
Spinrad, H., Marr, J., Aguilar, L., & Djorgovski, S. 1985, PASP, 97, 932
Sreekumar, P., Bertsch, D. L., Hartman, R. C., Nolan, P. L., & Thompson, D. J. 1999, Astropart. Phys., 11, 221
Stawarz, Ł., Kneiske, T. M., & Kataoka, J. 2006, ApJ, 637, 693
Stawarz, Ł., & Ostrowski, M. 2002, ApJ, 578, 763
Stawarz, Ł., Sikora, M., & Ostrowski, M. 2003, ApJ, 597, 186
Swain, M. R., Bridle, A. H., & Baum, S. A. 1998, ApJ, 507, L29
Taylor, G. B., et al. 2006, MNRAS, 368, 1500
Urry, C. M., & Padovani, P. 1995, PASP, 107, 803
Wilkinson, P. N., Akujor, C. E., Cornwell, T. J., & Saika, D. J. 1991, MNRAS, 248, 86
Wills, K. A., et al. 2004, MNRAS, 347, 771